ILASS–Europe 2017, 28th Conference on Liquid Atomization and Spray Systems, 6-8 September 2017, Valencia, Spain
http://dx.doi.org/10.4995/ILASS2017.2017.4685

Theoretical and Experimental Study of Grouping Effects on Droplet Streams

Norbert Roth[1*], Hassan Gomaa[1], Alon Livne[2], David Katoshevski[2], Bernhard Weigand[1]
[1]Institute of Aerospace Thermodynamics (ITLR), Universität Stuttgart, Germany
[2]Faculty of Engineering Sciences, Ben-Gurion University of the Negev, Israel
*Corresponding author: norbert.roth@itlr.uni-stuttgart.de

Abstract
Grouping of droplets was studied in monodisperse droplet streams. This very controllable system allows to study basic effects. In experiments droplet streams with monodisperse droplets were generated, however, with initially two different inter droplet spacing. A larger inter droplet spacing is followed by a little bit smaller one, which is followed by a larger one and so on. Due to this initial boundary condition groups of two droplets form, which approach each other and finally coagulate. It was found, that the velocity of the droplet approach is linearly dependent on the spacing between the droplets. This process was simulated by direct numerical simulation using the in-house code FS3D. The results of the simulations show the same linear behaviour. For larger computational domains the numerical results approach the experimental results.

Keywords
Droplet streams, Grouping effects, Shadowgraphy, Direct Numerical Simulation

Introduction

In spray systems a tendency to form groups can be observed [1, 2]. That has an influence on their evaporation, the drag force applied on them, their motion, and on their final settling point. This tendency has ramifications in energy and transportation systems as well as inhalation systems, paint and domestic sprays [3]. The better one understand the phenomenon of droplet grouping, the better one can control it and manipulate it tailored for each application, for instance to reduce fine particle emissions [4]. For better understanding the physics of droplet grouping processes, a well defined system of droplets is studied numerically and experimentally. An advantage of such systems is, that in the experiments the initial and boundary conditions are well known and can be controlled precisely. This allows a direct comparison between numerical calculations and experimental results. For this reason in a first approach monodisperse droplet streams are studied, which are produced by a droplet stream generator; the operation characteristics are described in [5]. Due to drag forces the velocity of the droplets in such a stream decrease as described below. Very small irregular disturbances in the initial inter droplet spacing a increase downstream until irregular groups form and finally droplets collide. In order to study basic grouping effects in detail it would be desirable to produce droplet streams with initially small, however, regular differences in inter droplet spacing. This is possible in modulation of the excitation signal of the droplet stream generator. Orme and Muntz suggested and described an amplitude-modulated excitation [6]. A theoretical description is given by Hilbing and Heister [7]. A detailed experimental and theoretical study of amplitude- and frequency-modulated excitation of droplet stream generators has been performed by Brenn und Lackermeier [8]. In this study here two frequency generators are used resulting in a frequency-modulated excitation. The details are described in the next section.

Material and methods

In Fig. 1 a schematic view of the experimental setup is shown including a photograph of the droplet stream generator used. In all experiments iso-propanol was used and the diameter of the orifice was $r_{orifice} \approx 60\,\mu\mathrm{m}$. In Fig 2 on the left hand side a so-called normal monodisperse droplet stream is shown schematically together with the indication of the parameters, which characterize the droplet stream. On the right hand side shadowgraphs of a normal droplet stream are presented, which show the building process of the monodisperse droplet stream. Using an appropriate excitation frequency f_s monodisperse droplet streams are obtained. In a first step an optimum frequency $f_{opt} = f_s = 49,800\,\mathrm{Hz}$ for the present experimental setup was determined using the method of self-stabilization presented on the DIPSI 2014 workshop in Bergamo [9]. In a second step the optimum of the initial droplet spacing $\lambda_{opt} \approx 294\,\mu\mathrm{m}$ was calculated according to the theory of Lord Rayleigh taking the properties of the droplet liquid, in this case iso-propanol, into account [10].In a third step the droplet generator was operated at the frequency f_s, the driving pressure was chosen to obtain an initial droplet spacing a_0 close to λ_{opt}. It is expected, that for this configuration an optimum in the regularity of the monodisperse droplet stream is obtained. In ongoing work tests concerning this topic are performed. Results for this normal droplet stream are presented below. Grouping effects were studied for the cases, when groups consisting of two droplets were generated. This was possible using two frequency generators. In the case n droplets were in one group the first frequency generator was running at the frequency $f_1 = f_s/n$. With this frequency $f1$ the second frequency generator running in a pulse mode was triggered. For each trigger pulse the second frequency generator sent n pulses at a frequency $f_2 > f_1$ to the droplet generator. Good results were obtained for $f_2 = 51,600\,\mathrm{Hz}$. The droplet generator produced then droplets of a temporal distance of $1/f_2$ seconds within a group and a temporal distance between the groups of $1/f_1 = n/f_s$

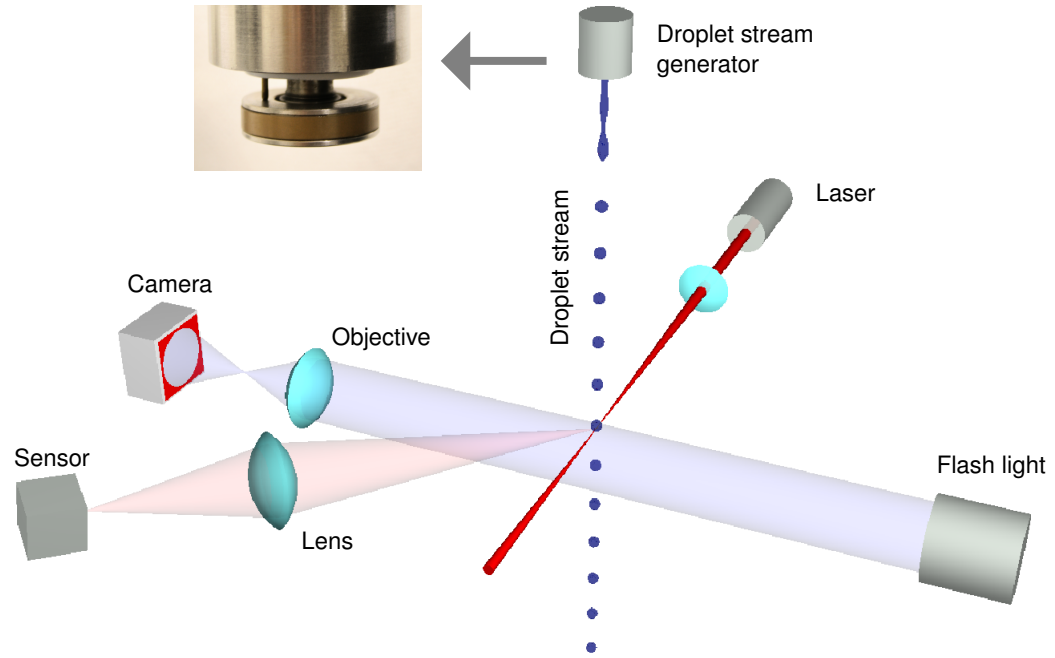

Figure 1. Schematic view of the experimental setup.

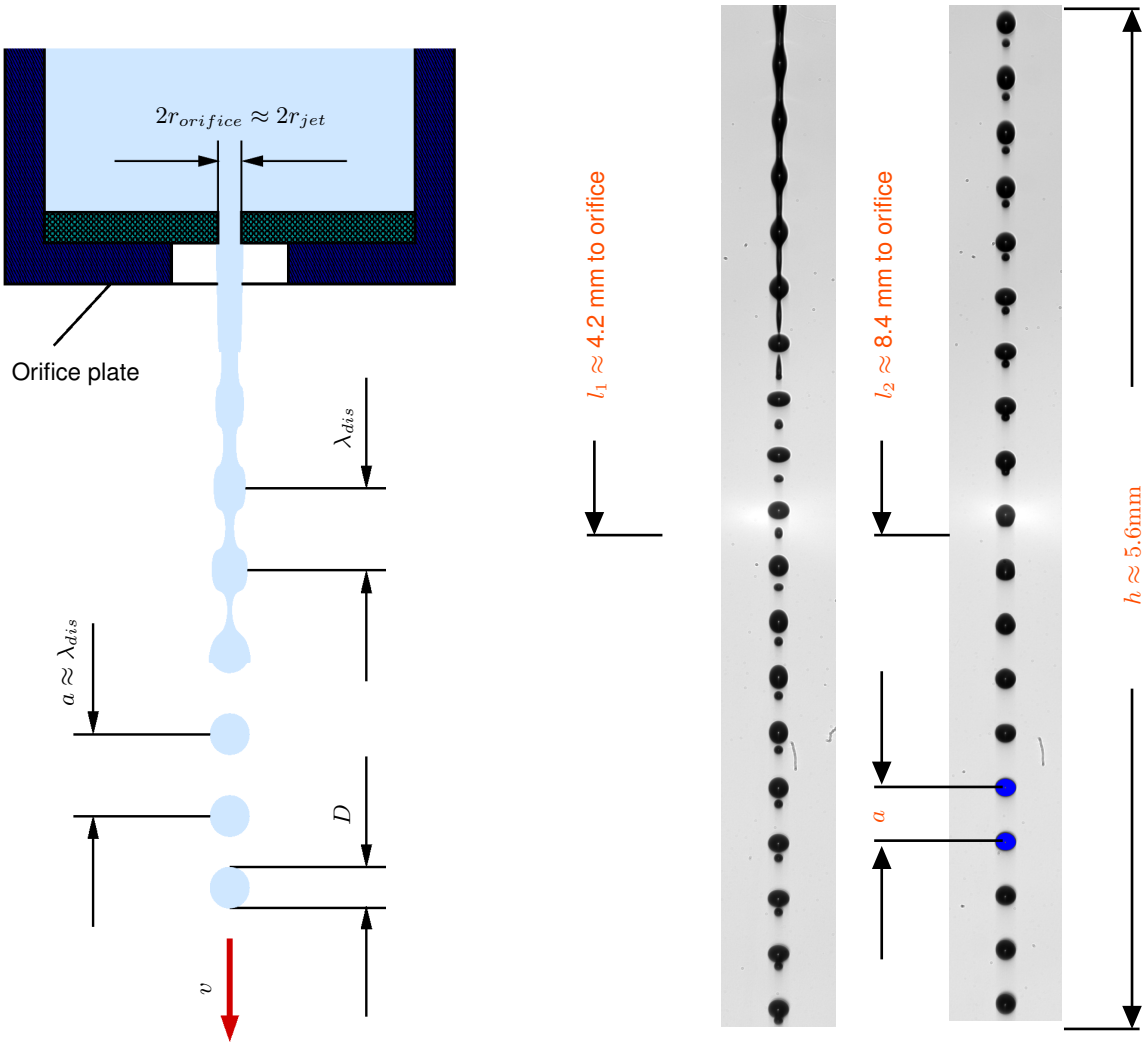

Figure 2. Schematic view of droplet generation indicating the parameters of a normal monodisperse droplet stream on the left hand side. Shadowgraphs of the normal droplet stream at two different distances l_i to the orifice plate on the right hand side.

seconds. Results for pairs ($n = 2$) of droplets are presented below. Each pair is forming a group. The spacing between the groups is denoted by g, the spacing between the droplets of the pair by a_2, and the spacing between the last droplet of the pair and the first droplet of the following pair by a_1. Therefore one obtains $g = a_1 + a_2$. The velocity of the droplet is obtained by $v = gf_1$. The droplet generator can be moved vertically in order to observe different positions l below the orifice plate. From shadowgraphs of the droplet stream taken by the camera the droplet size and the spacing between the droplets are determined. The sensor and the laser beam are used to monitor the passing by of each droplet and to help to adjust the droplet stream correctly. In all cases presented here the droplet diameter was $D \approx 112\,\mu\mathrm{m}$. Evaporation processes can be neglected. The initial values for the droplet distances are obtained from shadowgraphs taken at a position l, at which the droplets have formed completely. For the initial velocity the value $v_0 \approx 15.1\,\mathrm{m/s}$ was obtained. In the experiments the velocity of the droplets is decreasing along the droplet stream due to drag forces resulting in a decrease of the group distance g as the frequency f_1 of the group production remains constant.
If pairs of droplets are produced the droplets of a pair will collide further downstream. The colliding process was simulated numerically using an in-house program code named Free Surface 3D (FS3D). This code solves the incompressible Navier-Stokes equations. In order to take into account for the liquid phase the Volume-Of-Fluid (VOF) method is used. The free surface of the liquid phase is reconstructed by the Piecewise-Linear-Interface-Construction (PLIC) method. Further details can be found in [11]. For the simulation of the droplet stream periodic boundary conditions in the direction of motion were used. Four droplets have been simulated forming two pairs of droplets. Two slightly different spacing between the droplets were initialized in order to take into account of the two pairs of droplets. Using the data from the experiments a length of the computational domain in the direction of motion or x-direction of $d_x = 2g_0 = 1,211\,\mu\mathrm{m}$ was used. Two different widths of the computational domain were used, a smaller domain with $d_{yA} = d_{zA} = 300\,\mu\mathrm{m}$ (Case A: $512 \times 128 \times 128$ grid cells) and a wider domain with $d_{yB} = d_{zB} = 600\,\mu\mathrm{m}$ (Case B: $512 \times 256 \times 256$ grid cells). The first tests were performed with continuous boundary conditions at the side borders of the computational domain. This resulted in a drift of the droplet towards the side boundaries with finally leaving of the computational domain. Probably this was caused by an accumulation of the drift due to the periodic boundary conditions in the direction of motion. The droplets could be stabilized using walls with no-slip condition at the side boundaries. This condition, which is in contrast to the experiment, however, changed the behaviour of the droplets dramatically. An approach to the results of the experiments could be realized in widening the computational domain (case B). In analysing velocity profiles it can be seen, that the wider computional domain results in profiles, which are similar to simulations without walls. Results of the experiments and of the numerical simulations are presented in the following section. The numerical simulations with the wider domain have four times more grid cells resulting in a much longer CPU time.

Results and discussion

First a normal droplet stream with no initial formation of groups was studied. Using shadowgraphs the development of the spacing a between neighbouring droplets along the droplet stream was determined. The result is shown in Fig. 3. Due to drag forces the spacing a is decreasing along the droplet stream. Initial small irregularities in the spacing a increase along the droplet stream. If two droplet initially have a smaller spacing and the spacing to the neighbouring droplets is larger these droplet will approach each other and finally collide. This leads to an increase of the irregularities. The measurements were performed from top to bottom with gaps between the shadowgraphs taken. Afterwards the missing shadowgraphs were taken from bottom to top in order to check if changes occurred during the measurement. Due to the sensitivity to the boundary condition a small difference between both measurement series is observed. For the evaluation of the shadowgraphs the image processing tool ImageJ was used [12].

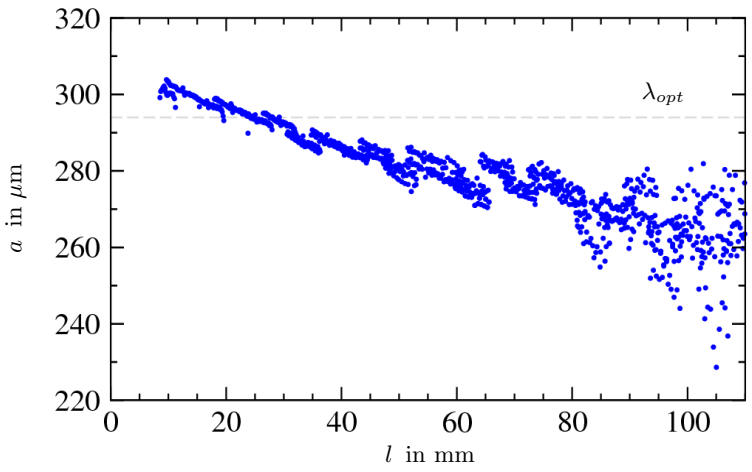

Figure 3. Space a between neighbouring droplets as function of distance l to the orifice plate of the droplet generator. The initial distance $a_0 \approx 300\,\mu\mathrm{m}$ is chosen to be close to the optimum λ_{opt} indicated by the grey dashed line. With an excitation frequency of $f_s = 49,800\,\mathrm{Hz}$ an initial droplet velocity $v_0 = a_0 f_s \approx 14.9\,\mathrm{m/s}$ is obtained.

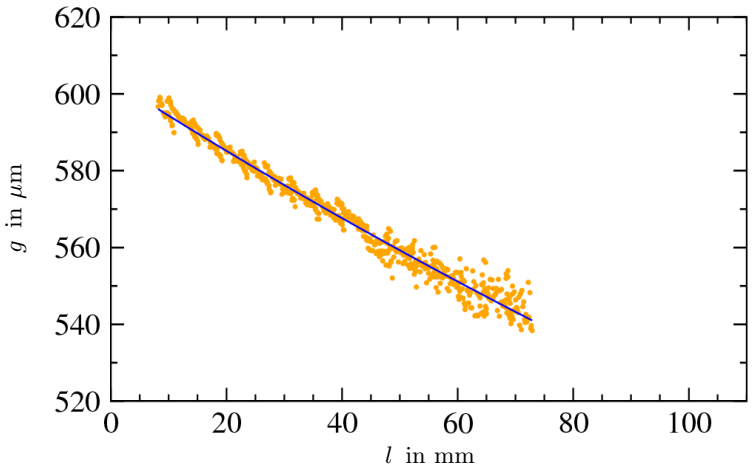

Figure 4. Spacing g between the droplet groups consisting of two droplets as function of distance l to the orifice of the droplet generator. The development of the droplet velocity v can be obtained by multiplying the spacing g by the frequency f_1 the groups are generated. The regression to the data is shown as solid line in the diagram.

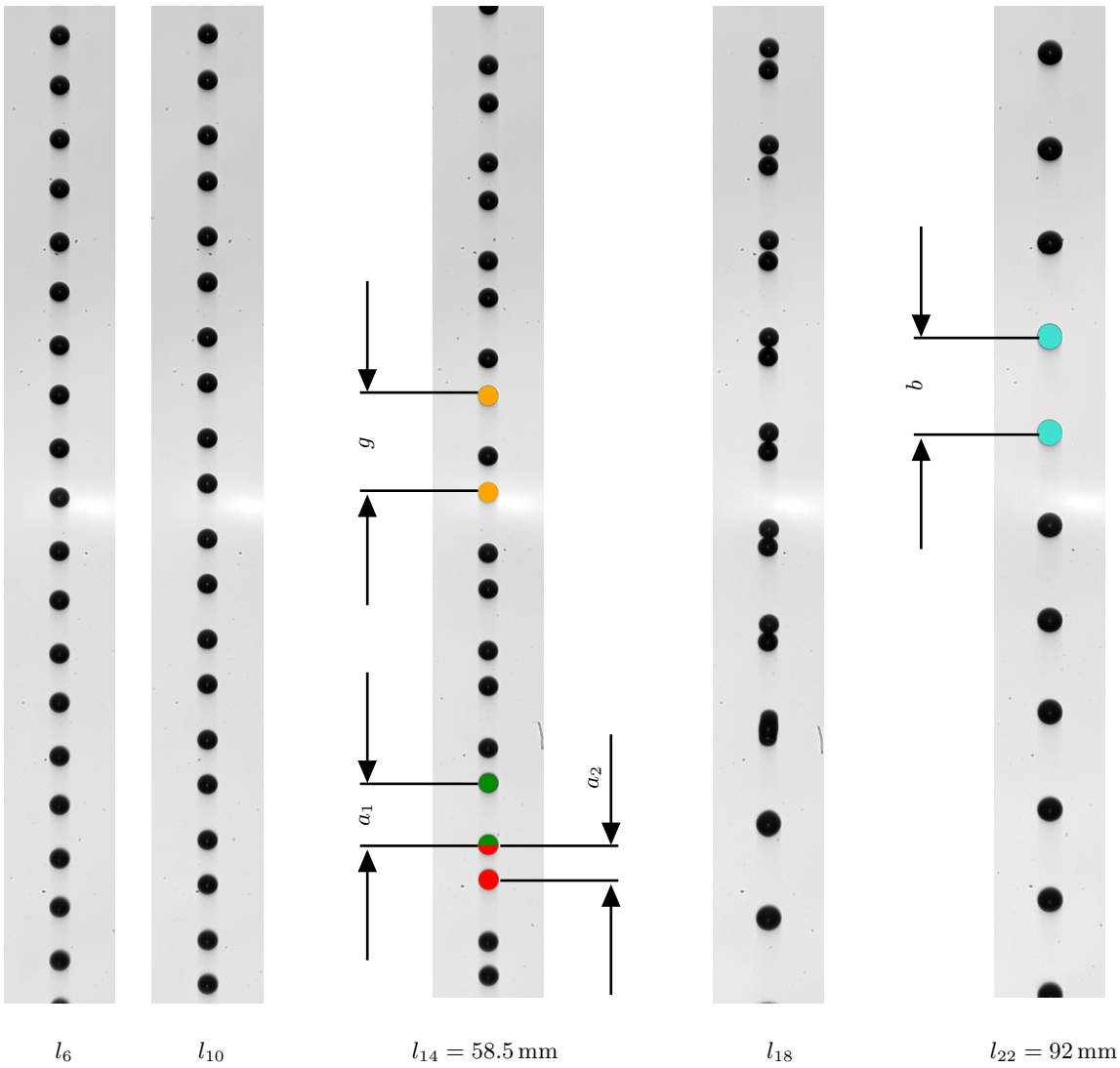

Figure 5. Shadowgraphs of the droplet stream at different distances l_i to the orifice plate. The distance l increases from left to right by $16.8\,\mathrm{mm}$ from image to image. For a better understanding of Fig. 6 the spacing a_i between neighbouring droplets before the coagulation of the two droplets of a group are indicated. The spacing b indicates the inter droplet spacing after the collision The spacing g indicates the spacing between neighbouring groups (group length).

The following measurements were performed on droplet streams with pairs of droplet generated initially as described above. The spacing g between the groups consisting of two droplets along the droplet stream is shown in Fig. 4. Again the shadowgraphs were evaluated as far as possible automatically using scripts developed using the image processing tool ImageJ. The behaviour of g is similar to the development of the spacing a in Fig. 3. The data obtained can be approximated by a regression function according to $v = 1/(p_3 + p_4 l)$ where p_3 and p_4 denote constants. Integration gives the time t a droplet needs to reach the distance l from the orifice plate. Shadowgraphs of the droplet stream at different distances to the orifice are shown in Fig. 5. For clarification all important spacing are indicated. These shadowgraphs give an overview of the approaching and collision process. In Fig. 6 the spacing a_i are plotted as a function of time t. The spacing seem to change exponentially. A regression with an exponential function $a_i = p_{5,i} \exp(p_{6,i} t) + p_{7,i}$ gives very good results with the constants $p_{j,i}$ taking into account the different inter droplet spacing. However, the data of a_1 and a_2 are not symmetrical to a horizontal line at $(a_{0,1} + a_{0,2})/2$ indicated by a dashed grey line in the figure. This is due to the decrease of the group spacing g shown in Fig. 4. If the spacing a_i are related to the actual inter group spacing g the values of the relative spacing a_1/g and a_2/g are symmetrical as can be seen from Fig. 7.

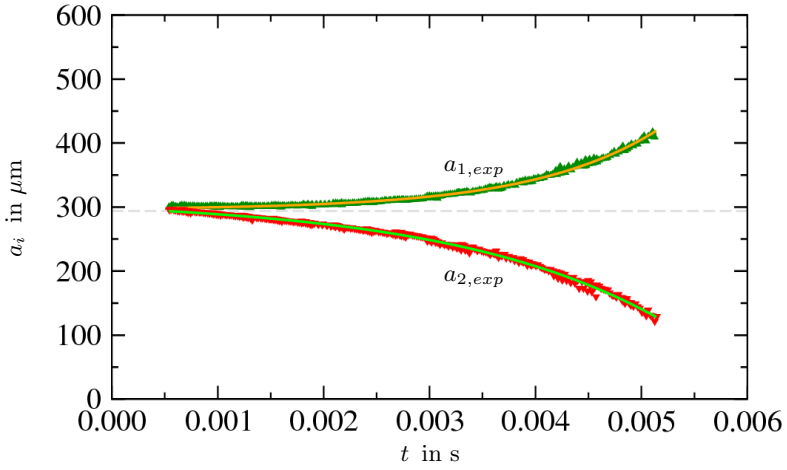

Figure 6. Spacing a_i between neighbouring droplets as a function of time t. The distance l was converted to the corresponding time t. The solid lines represent the exponential regressions to the data.

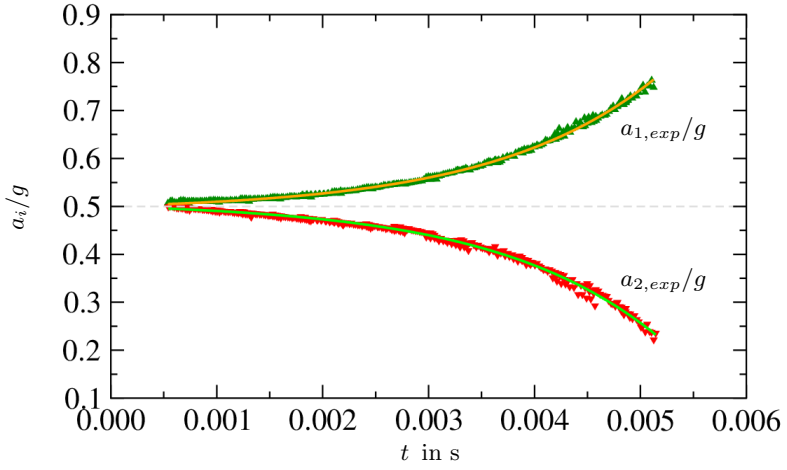

Figure 7. Relative spacing a_i/g as a function of time t. The solid lines represent the exponential regressions of the data.

Numerical simulations were performed of the grouping process as described above. Results for two different sizes (cases A and B) of the computational domain are presented in Fig. 8. The results are obtained in evaluating the results from FS3D with a MatLab code developed. Shown are the relative spacing a_i/g as a function of time t for both cases. In both cases the data can be approximated like the experimental data by an exponential function, which is represented by the black solid lines. A comparison of the numerical with the experimental results are shown in Fig. 9. Shown are the exponential regression of the data presented in Figs. 7 and 8. The numerical results approach the experimental results for a wider computational domain. Differentiating the exponential function $a_i/g = p_{8,i} \exp(p_{9,i} t) + p_{10,i}$ one obtaines the velocities $w_i = \partial(a_i/g)/\partial t = p_{9,i} p_{8,i} \exp(p_{9,i} t)$. These velocities indicate how fast the inter droplet spacing are changing. The velocities w_i as a function of time are shown in Fig. 10. Here too, the numerical results with a wider computational domain are closer to the experimental results. Substituting the time t by the relative distances a_i/g straight lines are obtained, which can easily be shown. This means that the

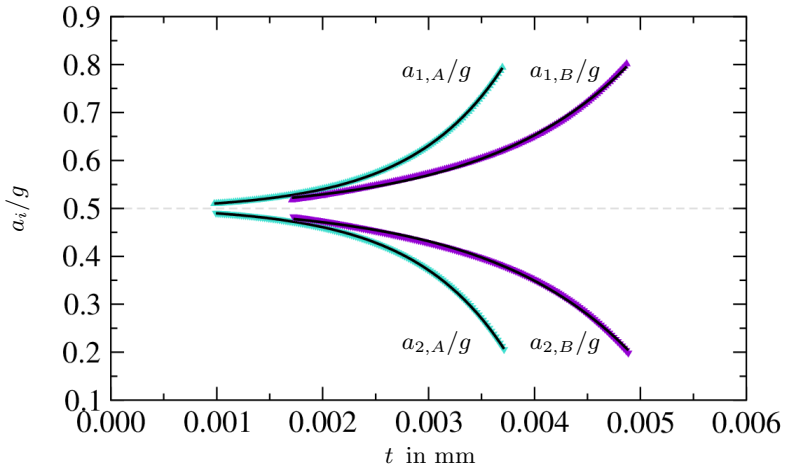

Figure 8. Relative spacing a_i/g as a function of time t. Shown are results of numerical simulations for different sizes of the computational domain (Cases A and B). The solid black lines represent the exponential regressions of the data.

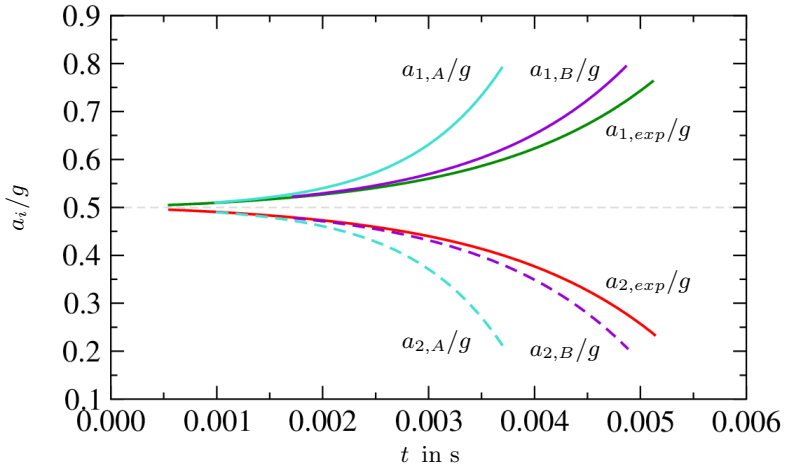

Figure 9. Relative spacing a_i/g as a function of time t. Shown are results of numerical simulations for different sizes of the computational domain (Cases A and B) in comparison with the experimental results (Index exp). All lines represent the exponential regressions of the data.

velocity w_i two droplets are approaching is a linear function of the relative spacing a_i/g between these two droplets. The results of this substitution is shown in Fig. 11. The comparison of numerical with experimental results shows the same trend, that for a wider computational domain the results of the numerical simulations are closer to the

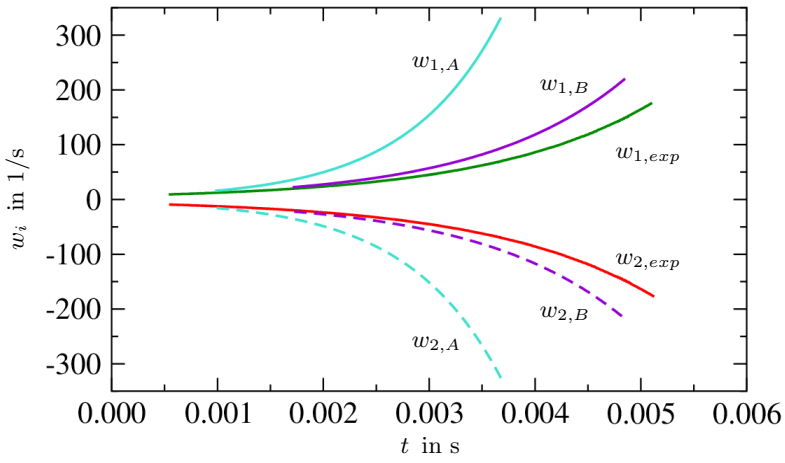

Figure 10. Velocities w_i as a function of time t. Shown are results of numerical simulations for different sizes of the computational domain (Cases A and B) in comparison with the experimental results (Index exp). All lines represent derivations of the exponential regressions to the data.

experimental results.

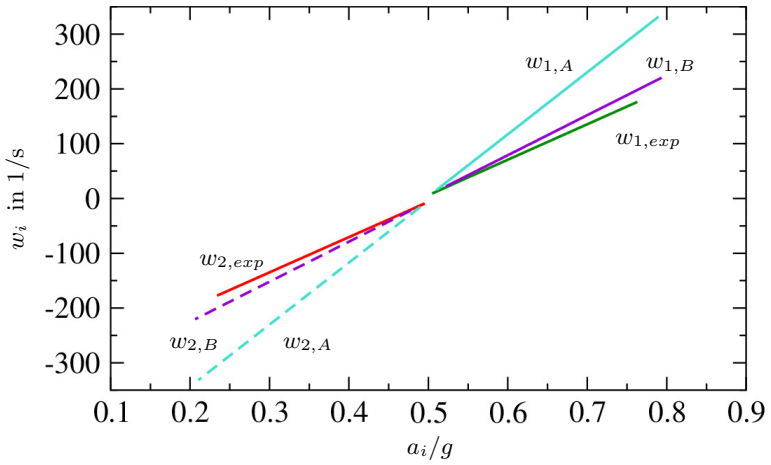

Figure 11. Velocities w_i as a function of time relative spacing a_i/g. Shown are results of numerical simulations for different sizes of the computational domain (Cases A and B) in comparison with the experimental results (Index exp). All lines represent derivations of the exponential regressions to the data.

Conclusions

Experiments and Direct Numerical Simulations were performed to study grouping effects in monodisperse droplet streams. It was described, how droplet streams with groups of two droplets can be generated experimentally. The setup for the simulation was presented. It was found, that the behaviour, how droplets within a group approach each other, can be approximated by an exponential law. Assuming such an exponential behaviour the velocity the droplet approach is a linear function of the actual distance between the droplets. This was found in the experiments as well as in the numerical simulations. In comparison of the simulations with the experimental results a wider computational domain show results, which are closer to the experimental results.

Acknowledgements

Nomenclature

D	droplet diameter [m]
a	inter droplet spacing [m]
b	inter droplet spacing after coagulation [m]
f_1	frequency of the group generation [Hz]
f_2	frequency of the droplet generation within a group [Hz]
f_{opt}	optimum wave frequency at Rayleigh disintegration [Hz]
f_s	excitation frequency [Hz]
g	spacing between the droplet groups [m]
d_i	dimensions of computational domain with $i = x, y, z$ [m]
l, l_i	distance to the orifice of the droplet stream generator [m]
n	number of droplets in a group [-]
p_3, p_4	parameters for the approximation of the velocity (various dimensions)
$p_{j,i}$	parameters for the exponential approximations, $j = 1 \text{ and } 2$, $i = 1 \text{ to } 5$ (various dimensions)
r	radius [m]
v	droplet velocity [m/s]
w	velocity the relative inter droplet spacing change [1/s]
Greek symbols	
λ	optimum wave length at Rayleigh disintegration [m]
Indices	
m	mass [kg]
a	acceleration [m s^2]
F	force [N]
m	mass [kg]

References

[1] J. Heinlin and U. Fritsching. Droplet clustering in sprays. *Experiments in Fluids*, Vol. 40, pp. 464–472, 2006.

[2] D. Katoshevski. Characteristics of spray grouping/non-grouping behavior. *Aerosol Air Quality Research*, Vol. 6, No. 10, pp. 54–66, 2006.

[3] D. Katoshevski, T. Shakked, S.S. Sazhin, C. Crua, and M.R. Heikal. Grouping and trapping of evaporating droplets in an oscillating flow. *International Journal Heat Fluid Flow*, Vol. 29, pp. 415–426, 2008.

[4] J. Gallego-Juaarez, E. Riera-Franco de Sarbia, G. Rodriguez-Corral, T.L. Hoffmann, and J. Gaalvez-Moraleda. Application of acoustic agglomeration to reduce fine particle emissions from coal combustion plants. *Environ. Sci. Technol*, Vol. 33, pp. 3843–3849, 1999.

[5] K. Anders, N. Roth, and A. Frohn. Operation characteristics of vibrating-orifice generators: The coherence length. *Part. Part. Syst. Charact.*, Vol. 9, pp. 40–43, 1992.

[6] M. Orme and E. P. Muntz. The manipulation of capillary stream breakup using amplitude-modulated disturbances: A pictorial and quantitative representation. *Physics of Fluids*, Vol. 2, pp. 1124–1140, 1990.

[7] J. H. Hilbing and S. D. Heister. Droplet size control in liquid jet breakup. *Physics of Fluids*, Vol. 8, pp. 1574–1581, 1996.

[8] G. Brenn and U. Lackermeier. Drop formation from a vibrating orifice generator driven by modulated electrical signals. *Physics of Fluids*, Vol. 9, pp. 3658–3669, 1997.

[9] N. Roth, H. Gomaa, and B. Weigand. Self-stabilization phenomena in the operation of droplet stream generators. DIPSI Workshop 2010 on Droplet Impact Phenomena & Spray Investigation, 2014.

[10] Lord J.S.W. Rayleigh F.R.S. On the instability of a cylinder of viscous liquid under capillary force. *Philos. Mag.*, Vol. 34, pp. 145–154, 1892.

[11] K. Eisenschmidt, M. Ertl, H. Gomaa, C. Kieffer-Roth, C. Meister, P. Rauschenberger, M. Reitzle, K. Schlottke, and B. Weigand. Direct numerical simulations for multiphase flows: An overview of the multiphase code fs3d. *J. of Applied Math*, Vol. 272, pp. 508–517, 2016.

[12] C.A. Schneider, W.S. Rasband, and K.W. Eliceiri. Nih image to imagej: 25 years of image analysis. *Nature Methods*, Vol. 9, pp. 671–675, 2012.